Journal Pre-proof

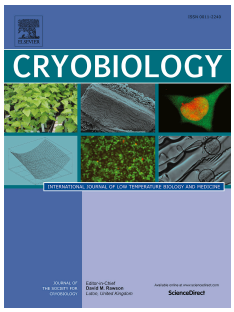

Effects of nanofibrillated cellulose hydrogels on adipose tissue extract and hepatocellular carcinoma cell spheroids in freeze-drying

Vili-Veli Auvinen, Arto Merivaara, Jasmi Kiiskinen, Heli Paukkonen, Patrick Laurén, Tiina Hakkarainen, Raili Koivuniemi, Riina Sarkanen, Timo Ylikomi, Timo Laaksonen, Marjo Yliperttula

PII: S0011-2240(19)30211-1

DOI: https://doi.org/10.1016/j.cryobiol.2019.09.005

Reference: YCRYO 4111

To appear in: *Cryobiology*

Received Date: 12 July 2019

Revised Date: 10 September 2019

Accepted Date: 10 September 2019

Please cite this article as: V.-V. Auvinen, A. Merivaara, J. Kiiskinen, H. Paukkonen, P. Laurén, T. Hakkarainen, R. Koivuniemi, R. Sarkanen, T. Ylikomi, T. Laaksonen, M. Yliperttula, Effects of nanofibrillated cellulose hydrogels on adipose tissue extract and hepatocellular carcinoma cell spheroids in freeze-drying, *Cryobiology* (2019), doi: https://doi.org/10.1016/j.cryobiol.2019.09.005.

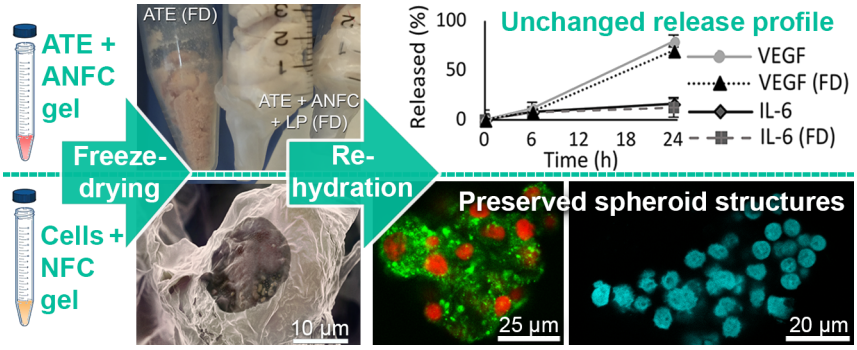

Effects of Nanofibrillated Cellulose Hydrogels on Adipose Tissue Extract and Hepatocellular Carcinoma Cell Spheroids in Freeze-Drying

Vili-Veli Auvinen[1,2] ¶, Arto Merivaara[1] ¶, Jasmi Kiiskinen[1], Heli Paukkonen[1], Patrick Laurén[1], Tiina Hakkarainen[1], Raili Koivuniemi[1], Riina Sarkanen[3], Timo Ylikomi[3], Timo Laaksonen[2], Marjo Yliperttula[*1,4]

[1]Division of Pharmaceutical Biosciences, Faculty of Pharmacy, University of Helsinki, P.O. Box 56, 00014 Helsinki, Finland
[2]Faculty of Engineering and Natural Sciences, Tampere University, P.O. Box 541, 33014 Tampereen yliopisto, Finland
[3]Faculty of Medicine and Health Technology, Tampere University, Kauppi Campus, Arvo Ylpön katu 34, 33520 Tampere, Finland
[4]Department of Pharmaceutical and Pharmacological Sciences, University of Padova, Via Marzolo 5, 35131 Padova, Italy

* Corresponding author
Email: marjo.yliperttula@helsinki.fi
Tel. +358 294159131
Viikinkaari 5E, P.O. Box 56, 00014, University of Helsinki, Helsinki, Finland

¶ The authors contributed equally to this work.

Abstract

The aim of this study was to evaluate the effects of two nanofibrillated cellulose (NFC) hydrogels on two human derivatives during freeze-drying. Native NFC hydrogel is a suitable platform to culture 3D cell spheroids and a hydrogel processed further, called anionic NFC (ANFC) hydrogel, is an excellent platform for controlled release of proteins. Moreover, it has been shown to be compatible with freeze-drying when correct lyoprotectants are implemented. Freeze-drying is a method, where substance is first frozen, and then vacuum dried trough sublimation of water in order to achieve dry matter without the loss of the original three-dimensional structures.

The first chosen human derivative was adipose tissue extract (ATE) which is a cell-free growth factor-rich preparation capable of promoting growth of regenerative cells. The release of growth factors from the freeze-dried mixture of ATE and ANFC was compared to that of non-freeze-dried control mixtures. The release profiles remained at the same level after freeze-drying. The second derivative was hepatocellular carcinoma (HepG2) cell spheroids which were evaluated before and after freeze-drying. The 3D structure of the HepG2 cell spheroids was preserved and the spheroids retained 18% of their metabolic activity after rehydration. However, the freeze-dried and rehydrated HepG2 cell spheroids did not proliferate and the cell membrane was damaged by fusion and formation of crystals.

Keywords: Nanofibrillated cellulose, freeze-drying, cell spheroids, adipose tissue extract, 3D cell culture

Abbreviations: NFC: Nanofibrillated cellulose; ANFC: Anionic nanofibrillated cellulose; ATE: Adipose tissue extract

Introduction

Nanofibrillated cellulose (NFC) is manufactured from natural biopolymer cellulose, and commonly wood pulp is used as a starting material [5,30]. Native NFC is biocompatible and non-toxic and has been proven to function as a scaffold in 3D cell culturing due to the fiber structure that mimics the collagen matrix of human tissue [5,39]. When cell suspension is mixed with the hydrogel, the cells autonomously form spheroids in the following days [5]. Native NFC can be further processed into anionic nanofibrillated cellulose (ANFC) for example trough TEMPO [(2,2,6,6-tetramethylpiperidin-1- yl)oxyl] oxidation [45,46]. The suitability of nanofibrillated cellulose in regenerative medicine and in controlled drug delivery has been shown [31-33,42]. In addition, ANFC can be freeze-dried and rehydrated without the loss of rheological properties [42].

Freezing, drying and rehydration are stressful processes for biological structures and especially for living organisms. However, freeze-drying has been shown to preserve protein pharmaceuticals, vaccines, plasma, platelets, red blood cells and sperm cells [18,22,24,54,57] and it is a widely used method for drying heat sensitive and biological materials in general. During freezing, osmotic pressure increases radically as any free water crystallizes. Changes in osmotic pressure and ice crystals can damage biological structures. However, the stress caused by freezing can be reduced by vitrification, which can be implemented in two ways, through extra rapid cooling [4,50] or by additives (cryoprotectants) [19]. Moreover, the damage caused by dehydration can be reduced by additives (lyoprotectants) [55].

The importance of additive trehalose for preserving liposomes, red blood cells and platelets in freeze-drying is well established [14,24,57]. In anhydrobiotic organisms the amount of trehalose is typically high [9]. In addition, intracellular trehalose appears to protect DNA integrity, mononuclear cells and retinal pigment epithelial cells [40,56,60]. It has been also reported that in addition to trehalose other excipients are required to dry mammalian cells [38,49]. Glycerol clusters water into smaller compartments, reducing the formation of large ice crystals [52]. Cellulose fibers and polyethylene glycol (PEG) are hygroscopic polymers and hence improve the uptake of water at the rehydration phase while providing mechanical support to the aerogel [8,27]. Due to several hydroxyl groups and rigid carbon bone, cellulose fibers are known to provide structural and physicochemical support during freezing and sublimation phases of freeze-drying [2,26]. However, the effects of wood derived nanocellulose fiber network on human derivatives during freeze-drying has not yet been studied.

The first chosen human derivative in our study was adipose tissue extract (ATE) which is a cell-free, growth factor-rich preparation. It is inexpensively obtained through a simple lipoaspirate method [35]. The concentration of the growth factors in ATE varies between the patients and the extraction sites due to factors such as body mass index and age. However, the variation can be decreased by optimized liposuction and extraction method [35]. ATE has been demonstrated to promote wound healing properties in *in vitro* models [34,47] and in animal models [23] and has been studied with a new versatile human vascularized adipose tissue model [25]. It has potential applications and ongoing studies on the medical field due to the growth factors found in it naturally, yet one of the challenges is the adequate spatio-temporal delivery of growth factors [44]. As the adipose tissue extract is mostly composed of proteins and water, in

this study we observed the release of two important proteins. The chosen proteins were vascular endothelial growth factor (VEGF-A, anionic at pH 7) and interleukin 6 (IL-6, ~neutrally charged at pH 7) which are angiogenesis inducing growth factors [7,47]. The protein release was measured before and after freeze-drying, to compare the release of model proteins between freshly mixed hydrogel formulations and freeze-dried hydrogel formulations after rehydration.

The second human derivative was 3D cultured hepatocellular carcinoma (HepG2) cell spheroids. In the experiment, their enzymatic and metabolic activity and morphology were compared before and after freeze-drying in native NFC hydrogel. In general, 3D tumor spheroids operate as exceptional models for drug research [6,37,41] and predict drug toxicity with increased accuracy over traditional 2D cell cultures [43]. Traditional 2D cultured cells might have altered phenotypes which differ from tissues and in vivo organs and might produce misleading results [37]. 2D cultured cells lack the cell-cell and cell-extracellular matrix signaling which is vital for cells in 3D environment for cell proliferation and differentiation [6]. The 3D cell spheroid cultures resemble *in vivo* environment and they could be used as a link between *in vitro* and *in vivo* experiments in drug discovery. Accurate drug toxicity predictions during pre-clinical phases of medical development spares resources and lives of test animals. However, production and upkeep of 3D cell cultures consume time and resources compared to traditional cell culturing methods. In addition, transportation, storage and usability of such cell products require improvement in general. Our aim was to gain new insight on the effects of NFC hydrogels during freeze-drying on cell spheroids in order to create a paradigm for resolving such issues in future studies.

Materials and Methods

Materials

The human adipose tissue extract (ATE) was obtained from Tampere University Hospital, Tampere, Finland, with individual written informed consent from a single patient during one operation of liposuction procedure. The use of ATE was approved by the Ethics Committee of the Pirkanmaa Hospital District, Tampere, Finland, with permit number R15161. The ANFC hydrogel (lot 11888-3) containing 6.55% (m/v) of fiber, the sterile native NFC hydrogel (GrowDex®, lot 11792) containing 1.5% (m/v) of fiber and sterile GrowDase™ cellulase enzyme mixture (lot 15002) were kindly provided by UPM-Kymmene Corporation, Finland. All the materials and chemicals used were of analytical grade and sterilized either by UV light, autoclave or filtration prior to implementation. D-(+)-trehalose dihydrate, low adhesion 96-well inertGrade BRANDplates®, Cellstain double staining kit, fetal bovine serum (FBS) and glycerol (99%), Human IL-6 ELISA Reagent Kit, Human VEGF-A ELISA Reagent Kit, sodium carbonate-bicarbonate, potassium chloride, sodium chloride, potassium phosphate, paraformaldehyde (PFA, 4%), Triton X-100 solution (10%), Tween 20 detergent, glycine (99%), Nunc Maxisorp 96-well ELISA Plates, Bovine Serum Albumin (BSA) and Trizma base (99.9%) were purchased from Sigma-Aldrich, USA. Polyethylene glycol 6000 (PEG 6000) was purchased from Fluka, Switzerland. Penicillin-streptomycin solution (P/S; 10 000 U/ml), Dulbecco´s modified eagle medium (DMEM) with high-glucose, L-glutamine and phenol red and Dulbecco's Phosphate Buffered Saline (DPBS) 10x concentrate without magnesium and calcium were purchased from Gibco, UK. Liquid nitrogen used in vitrification was purchased

from AGA Industrial Gases, Finland. PS SensoPlate™ 96 well glass bottom plates for confocal imaging were purchased from Greiner Bio-One, Austria. Cell culture flasks (25 and 75 m^2) were purchased from Corning, USA. The human liver hepatocellular carcinoma HepG2 cells (passage number 100, ATCC HB-8065) were purchased from ATCC®, USA. The 10 ml sterile syringes were purchased from Terumo, Japan. TrypLE Express, ProLong Diamond Antifade Mountant by Life Technologies, Chamber Slide™ system 8-well Permanox slide plates by Nunc™ Lab-Tek™, alamarBlue® Cell Viability Reagent by Invitrogen and Alexa Fluor 488 phalloidin were purchased from Thermo Fisher Scientific, USA. All solutions used were prepared in ultrapure water. ACS reagent (Sigma-Aldrich, Germany) was used to prepare 2 % anthrone solution in concentrated sulphuric acid (Sigma-Aldrich, Germany).

Preparation of the formulations of ATE and ANFC hydrogel

ATE was collected as described by Lopez et al. (2016) and obtained extracts were pooled together [35]. The ANFC hydrogel was homogenized with ATE and lyoprotectants (Fig 1A). 6.55% ANFC hydrogel was diluted with ATE, and the amount of fibers and lyoprotectants were scaled to the volume of ANFC hydrogel as in our previous studies resulting in 3% (m/v) of ANFC fiber, 53% of ATE (v/v), 0.5% (m/v) of PEG 6000 and 0.2% (m/v) of trehalose in the final formulation [42].

HepG2 cell cultures

HepG2 cells were cultured in DMEM with 10% (v/v) FBS and grown in T75 flask at 37 °C and 5% CO_2. The cells were divided every 3-4 days by first trypsinizing them with 4 ml of

TrypLE Express for 10 minutes, then adding 8 ml of fresh media and centrifuging cells for 5 minutes at 200 RFC. Lastly, the supernatant was aspirated, and the formed pellets were resuspended into DMEM with 10% (v/v) FBS and divided at a ratio of 1:4.

HepG2 cell spheroid cultures

HepG2 cell spheroids were grown for 4 or 7 days prior to freeze-drying at 37 °C and 5% CO_2. At the seeding phase, the 2D cell cultures were detached, collected and counted and the obtained cell suspension was diluted to achieve a final cell density of 7 x 10^5 cells/100 µl. Next, a desired volume of 1.5% native NFC hydrogel was pipetted into a polypropylene tube. Then, DMEM supplemented with 10% (v/v) FBS and the diluted cell suspension were mixed to the native NFC hydrogel to achieve a suspension with concentration of 0.8% (m/v) NFC fibers. 100 µl of the suspension was seeded to low attachment 96-well plate wells and an equal volume of media was added on top of each well.

Optimization of trehalose loading into HepG2 cell spheroids

To determine a suitable concentration of trehalose for the freeze-drying formulation, HepG2 cell spheroids were incubated with different trehalose concentrations for 24 hours. The cells were cultured in 0.8% (m/v) of native NFC hydrogel for 4 days before studying the effects of trehalose. The studied concentrations were 0 mM, 50 mM, 100 mM, 200 mM, 500 mM and 1000 mM. After loading the HepG2 cell spheroids with trehalose, their viability was determined with cellstain double staining kit and the spot detection tool of Imaris 9 -software by Bitplane,

United Kingdom. The evaluated viability was standardized to the viability of spheroids incubated with 0 mM trehalose.

Freeze-drying protocol

24 hours prior to freeze-drying, the cell culture media was changed to customized lyoprotective media containing 1% (m/v) glycerol, the concentration of trehalose as stated above and penicillin-streptomycin solution 1% (v/v). The layer of media and 0.8% (m/v) of native NFC hydrogel containing HepG2 cell spheroids in each cell culture well were mixed by pipetting to form a 0.4% (m/v) native NFC hydrogel. Control HepG2 cell spheroid samples were prepared by removing the NFC hydrogel via enzymatic digestion which was initiated with a 0.05% (m/v) cellulase enzyme mixture a day before freeze-drying. The obtained suspensions of HepG2 cell spheroids in native NFC hydrogel were snap frozen by injecting them as 20-200 µl droplets into UV-sterilized liquid nitrogen.

The frozen samples were transferred into a freeze-drying chamber of ScanVac CoolSafe manufactured by Labogene, Denmark. The pressure in the freeze-drying chamber was decreased to 0.001 mBar and the samples were dried for 72 hours. At the end of the cycle the dryness of the HepG2 cell spheroid samples was confirmed by observing the change of color of phenol red in DMEM as it turns yellow when free water is not present.

The mixtures of ATE, ANFC hydrogel and lyoprotectants were kept inside 10 ml syringes while frozen in liquid nitrogen. The samples were freeze-dried with ScanVac CoolSafe as above.

Rehydration and prehydration

Two different rehydration methods were studied: rehydration and prehydration. The rehydration was studied via addition of liquid rehydration solution, and the prehydration was studied via a combination of vapor and liquid.

The freeze-dried HepG2 cell spheroid samples were sealed with plastic film and incubated for 30 minutes in three different temperatures (4 °C, 25 °C and 40 °C). The rehydration solution contained ultrapure water, media and P/S antibiotics (79:20:1). The samples were rehydrated gravimetrically (+25% (v/v) to achieve the original osmotic pressure and the temperature of the rehydration solution was adjusted to match the temperature of each sample.

The effects of prehydration were studied by first incubating samples in saturated air-humidity for 30 min, 60 min and 90 min. Next, gravimetric rehydration was applied to the samples. Finally, all HepG2 cell spheroid samples were seeded to low attachment 96-well plates and incubated in 37 °C, 5% CO_2 incubator for 2 hours before staining.

After rehydration, the freeze-dried ATE and mixtures of ATE and ANFC aerogels were gravimetrically rehydrated and homogenized by mixing with two connected syringes as shown in Fig 1A.

Release studies of VEGF-A and IL-6 from ANFC hydrogel

Release studies were performed with the mixtures of ATE and ANFC hydrogels before and after freeze-drying. In both settings, the homogenization was performed by mixing with two attached syringes (Fig 1 A). The mixtures had a constant flat surface area of 2.01 cm^2 exposed to

500 µl of pH adjusted DPBS (Fig 1 B). The sink conditions were met. The samples were shaken on a plate shaker at 37 °C for 6 or 24 hours with 100 RPM (Fig 1 C), collected and analyzed with ELISA protein quantitation kits according to the manufacturer's instructions. The absorbance was measured with a plate reader (Varioskan Flash, Thermo Fisher) at 450 nm by subtracting the control value measured at 550 nm. Release results were scaled to the amount of growth factors in freeze-dried ATE and six parallel samples were measured in each setting.

Viability studies of freeze-dried HepG2 spheroids

Viability of freeze-dried HepG2 cell spheroids was evaluated by cell membrane integrity and metabolic activity. Untreated HepG2 cell spheroids were used as positive controls and HepG2 cells lysed with 70% ethanol as negative controls.

Cell membrane integrity was studied with Calcein AM and propidium iodide (PI) which were diluted in DPBS and delivered to HepG2 cell spheroids by incubating for 15 minutes in 37 °C and 5% CO_2. Samples were imaged with Leica TCS SP5 II HCS-A confocal microscope (Leica, Germany) by using argon 488 nm and DPSS 561 nm lasers with QD 405/488/561/633 splitter. Excitation of 488 nm with emission bandwidth of 498-535 nm were used to detect calcein (green) and excitation of 561 nm with emission bandwidth of 589-679 nm were used to detect PI (red).

Metabolic activity was evaluated by the cells' ability to convert resazurin to resorufin. A metabolic activity assay was implemented twice before and three times after freeze-drying on

days 1 and 3, and on days 7, 10 and 14, respectively. Resazurin was added as 10% (v/v) and incubated for four hours. After the incubation, 70 µl of media was collected to a black plate and the fluorescence was measured with Varioskan LUX (excitation 560 nm, emission 590 nm). Fluorescence signal was normalized to that of the control HepG2 cell spheroids on day 1.

Calcein AM compartmentalization study

To evaluate the behavior of calcein in cells with damaged cell membrane, control cells were permeabilized with Triton X-100 and stained with Calcein AM and PI. Staining was performed according to the manufacturer's instructions and the cells were seeded on an 8-well plate. Three experimental settings were conducted. In the first setting, control cells were first loaded with calcein AM and then permeabilized with Triton X-100 for 5 min, 10 min or 15 min to observe possible leakage of calcein. In the second setting, control cells were simultaneously permeabilized and stained to simulate the leakage occurring during the calcein AM staining. In the third setting, control cells were first permeabilized with Triton X-100 for 10 minutes and then stained to evaluate the behavior of calcein AM in cells with porous membranes. Measurements were performed in triplicates.

Evaluation of cell morphology and 3D structures of spheroids

To evaluate the effects of freeze-drying on the morphology of cell spheroids, filamentous actin cytoskeleton (F-actin) was stained with phalloidin Alexa 488 and nuclei with Hoechst 33342. For this experiment, cells were cultured as previously described, except the native NFC fibers were enzymatically digested to prevent unwanted binding of stains. The digestion was

initiated with a 0.05% (m/v) cellulase enzyme mixture a day before their fixation. The cell spheroids were fixed with 4% PFA for 20 minutes. PFA was washed three times with 0.1% (v/v) Tween 20 in DPBS. Cells were stored in the wash buffer on a plate rocker at 4 °C.

Before staining, HepG2 cell spheroids were permeabilized with 0.1% Triton X-100 in DPBS for 10 min. Blocking was performed with 0.1% (v/v) Tween 20 DPBS containing 1% (m/v) BSA and 0.3 M glycine for 30 minutes on a rotator. Phalloidin Alexa 488 (1:40 in 0.1% (v/v) Tween 20 DPBS containing 1% (m/v) BSA was added and the HepG2 cell spheroids were incubated overnight at 4 °C on a plate rocker. The following day the spheroids were placed on a microscopy glass to dry. Remaining phalloidin Alexa 488 was washed three times with the wash buffer and once with 0.1M Tris pH 7.4 solution. Nuclei were stained with Hoechst 33342 for 5 min. Hoechst 33342 was washed with 0.1M Tris pH 7.4 solution and spheroids were mounted with ProLong Diamond Antifade Mountant. The HepG2 cell spheroids were imaged with Leica TCS SP5 confocal microscope by using argon 488 nm and UV diode 405 nm lasers with QD 405/488/561/633 splitter. Excitation of 488 nm with emission bandwidth of 500 - 550 nm were used for phalloidin Alexa 488 and excitation of 405 nm with emission bandwidth of 415 - 470 nm were used for Hoechst 33342. Images were analyzed with Imaris 9 software.

HepG2 cell spheroids were imaged with a scanning electron microscope (SEM) to study the effects of freeze-drying on the morphology and the structure of the cell spheroids. In another setting, freeze-dried HepG2 cell spheroid samples were rehydrated and freeze-dried again to evaluate the effects of rehydration on the integrity of cell membrane.

The SEM samples were stored in a desiccator at 4 °C until imaged. The samples were not coated nor fixed for the SEM imagining which was performed with FEI Quanta 250 Field Emission Gun SEM using 2.0 kV and 2.5-3.0 spot in high vacuum.

Statistical analysis

Statistical analysis was performed with IBM SPSS Statistics 24 -software (IBM Corporation, USA). Statistical significance was determined with independent samples t-test, where $p<0.05$ was considered significant. The lethal concentration 50 value for trehalose media was determined by using regression probit analysis.

Results

Release of VEGF-A and IL-6 from ANFC hydrogel before and after freeze-drying

The measured amounts of growth factors in pooled untreated ATE were 187.0 µg/ml (±30) of VEGF-A and 193.1 µg/ml (±11) of IL-6 (n=6). After freeze-drying and gravimetric rehydration of the ATE, the measured amount of IL-6 stayed intact, while the amount of VEGF-A decreased to 105 µg/ml. However, when ATE was freeze-dried with ANFC and lyoprotectants, the amount of VEGF-A remained unchanged.

In the release studies before freeze-drying, 79.5% (±14.2) of VEGF-A and 16.4% (±7.9) of IL-6 was released from a mixture of ATE, ANFC hydrogel and lyoprotectants at the 24-hour time point (Fig 2A). No swelling of the hydrogel nor burst release were observed. However, after

freeze-drying and gravimetric rehydration of the mixture, similar release was observed in an identical setup. There, a 70% (±15.7) release of VEGF-A and a 12.6% (±5.4) release of IL-6 was detected at the 24-hour time point and the difference was not statistically significant ($p>0.05$). When freeze-dried, ATE formed a solid red cake and mixtures of ATE, ANFC hydrogel and lyoprotectants formed sturdy aerogels (Fig 2 B). The amount of sublimation and desorption water during the freeze-drying process of untreated ATE was 98.5% (m/m).

The effect of trehalose loading on cell viability

After 24 hours of incubation, standardized viability of HepG2 cell spheroids was 100% when 0 mM, 50 mM or 100 mM trehalose media were used. Higher concentrations of trehalose lead to lower cell viabilities. 200 mM concentration resulted in 78.7% viability (±1.8), 500 mM resulted in 16.1% viability (±1.2) and 1000 mM resulted in 5.1% viability (±0.9) (Fig 3). In addition, the higher concentrations of trehalose lead to the breakage of HepG2 cell spheroids into tinier units or single cells.

Effects of freeze-drying, rehydration and prehydration on cell membrane integrity

HepG2 cell spheroids which were freeze-dried in NFC matrix and stained with calcein AM and PI after rehydration emitted both green and red fluorescence (Fig 4). HepG2 cell spheroids freeze-dried without NFC matrix in suspension showed similar green fluorescence as the HepG2 cell spheroids freeze-dried with the NFC matrix (Supplementary material). Green fluorescence was observed in complete spheroids when incubated with 0 mM trehalose media (Fig 4.A) and

342 the intensity of green fluorescence was increased when cells were incubated with 50 mM
343 trehalose media (Fig 4B). The HepG2 cell spheroids loaded with 300 mM trehalose media prior
344 to freeze-drying showed higher intensity of green fluorescence than HepG2 cell spheroids freeze-
345 dried without trehalose or with low concentrations of trehalose (Fig 4C). However, the HepG2
346 cell spheroids loaded with 300 mM trehalose media broke into single cells (Fig 4C). When single
347 cells were freeze-dried in NFC hydrogel minor green fluorescence was observed while single
348 cells freeze-dried without native NFC hydrogel emitted only red fluorescence (Supplementary
349 material).
350
351 After rehydration, both green and red fluorescence were observed from single individual
352 cells in cell spheroids. Moreover, the observed green fluorescence appeared in granular
353 formations (Fig 5 A). In addition, overall intensity was measured to be significantly lower.
354 Similar results were obtained despite the concentration of trehalose or rehydration temperature.
355 The HepG2 cell spheroids that were rehydrated at 40 °C showed a minor increase in the intensity
356 of green fluorescence (Fig 5A) when compared to cell spheroids rehydrated at 4 °C (Fig 5B).
357
358 Prehydration of the HepG2 cell spheroid aerogels in saturated air humidity lead to
359 insufficient hydration. Only 2% (v/v) of original water content was reached regardless of the
360 time (30, 60 or 90 minutes). In addition, the freeze-dried cakes collapsed during the prehydration
361 and rehydrated insufficiently. No green fluorescence was observed.
362
363 The control cells permeabilized with Triton X-100 before staining showed green
364 fluorescence in granular formations similarly to freeze-dried and rehydrated samples (Fig 5 A

365 and C). Some of these permeabilized control cells were fully viable. Control cells permeabilized
366 and stained simultaneously prior to imaging showed similar granular green fluorescence and
367 decreased overall intensity of the green fluorescence as freeze-dried and rehydrated cells (Fig 5
368 B and D). Control cells loaded with calcein AM prior to permeabilization mostly detached from
369 the surface of the well plate and both green and red fluorescence was observed.
370
371

372 **Effects of freeze-drying and rehydration on metabolic activity and**
373 **on the morphology of the HepG2 cell spheroids**

374 Freeze-dried and revived HepG2 cell spheroids showed 18.1% (±6.1, n=8) of the metabolic
375 activity of the day 1 control samples on the day of revival (Fig 6A). However, the activity
376 decreased rapidly on the following days. The metabolic activity of the control HepG2 cell
377 spheroids remained stable over the test period (14 days). Similar results were obtained from
378 spheroids, which were freeze-dried on day 7. Their metabolic activity was 17.8% (±9.0, n=6) of
379 their day 1 controls' activity on the rehydration day.
380

381 The shape and the size of the rehydrated HepG2 cell spheroids resembled the control
382 spheroids. Immunocytochemistry staining with phalloidin Alexa 488 and nuclear staining with
383 Hoechst 33342 revealed that actin could be detected only prior to freeze-drying (Fig 6B and 6C).
384 In addition, the size of the nuclei decreased when the samples were freeze-dried and rehydrated
385 (Fig 6C). The nuclei size (n=42) reduction was statistically significant in Students' independent
386 sample t-test where $p<0.05$ was considered as significant. The reattachment of the freeze-dried

and rehydrated HepG2 cell spheroids was nearly non-existent, and the cells were incapable of proliferation.

Highly porous structures of freeze-dried native NFC aerogel were observed with SEM (Fig 7 A). Freeze-dried HepG2 cell spheroids maintained their shape and size without collapsing (Fig 7 B). Microvilli and membrane structures were observable, and the surface of the cell membrane appeared intact (Fig 7 C). Minor hornification was observed in NFC fibers that were freeze-dried only once (Fig 7 A, B and C). Major hornification and complete destruction of cells were observed in samples that were freeze-dried, rehydrated and freeze-dried again (Fig 7 D). Glycerol can be observed as smooth orbs with a diameter of approximately 10 μm (Fig 7 A and D).

Discussion

In our previous study, 32% of BSA (anionic at pH 7) was released from ANFC during the first 24 hours both before and after freeze-drying [42]. In the current study, IL-6 (~neutrally charged at pH 7) was released from ANFC hydrogel at a slower rate as expected. VEGF-A (anionic at pH 7) was released similarly as anionic model compounds ketoprofen and BSA in our previous study [42]. However, when compared to a VEGF release study with extracellular matrix mimicking gelatinous protein mixture hydrogel (Matrigel™) [17], the cumulative release of VEGF-A from ANFC was observed to be higher. This is due to the anionic nature of ANFC hydrogel which expedites the diffusion of negatively charged VEGF-A particles. Moreover, when large proteins diffuse through ANFC hydrogel, the charge of the molecule might be a more

410 significant factor than the size [42]. The effects of the lyoprotectants PEG 6000 and trehalose to
411 the release properties of ANFC are not significant, as we have shown earlier [42]. The freeze-
412 drying of ANFC did not alter the release rate of the model growth factors significantly.
413
414 In our experiments the freeze-dried, rehydrated and stained HepG2 cell spheroids emitted
415 red and green fluorescence simultaneously. Typically, in the dual staining viability studies, green
416 fluorescence indicates enzymatic activity, while red fluorescence indicates damaged cell
417 membrane. The calcein appeared compartmentalized and the intensity of its green fluorescence
418 was lower when compared to healthy control samples. Similar observations were made with the
419 Triton X-100 permeabilized cells. This suggests that the cell membrane of freeze-dried and
420 rehydrated HepG2 cell spheroids is damaged similarly as in the case of cell permeabilizing
421 agents. Furthermore, the calcein compartmentalization indicates that calcein is leaking out from
422 the cytosol [15]. Calcein accumulates in endosomes, lysosomes and mitochondria [51], which
423 can be observed as compartmentalized green fluorescence. However, calcein AM enters those
424 organelles mainly in case of slow or non-existent de-esterification [51]. If calcein enters
425 mitochondria, it indicates that the permeability of mitochondria is increased which is important
426 in cellular calcium homeostasis, autophagy, apoptosis and necrosis [29]. The higher observed
427 intensity of green fluorescence in cell spheroids rehydrated at 40 °C might be due to naturally
428 higher activity of enzymes in higher temperatures. The observed 18% metabolic activity
429 indicates that the mitochondria of freeze-dried and rehydrated HepG2 cell spheroids are still
430 functional on the revival day to some extent. By combining the observations of
431 compartmentalization and mitochondrial activity, we suggest that the previously mentioned cell
432 organelles are partially preserved during freeze-drying and rehydration. In addition, the

433 measured decrease in metabolic activity after the revival day indicates that the cell membranes
434 are damaged, yet the mitochondria are partly functioning for a short period of time. It appears
435 that the presence of NFC itself did not have any positive effects on the survivability of the cells,
436 however the 3D structure of the cell spheroids formed with the aid of native NFC hydrogel had a
437 significant impact on preserving cell structures.
438
439 The intracellular trehalose concentrations observed in this study (Supplementary material)
440 were low compared to literature [24,57]. Increase of the trehalose concentrations in the media
441 resulted in cell death due to hyperosmotic conditions. To achieve higher concentration of
442 intracellular trehalose, other loading methods such as freezing induced loading [59] or
443 acetylation of trehalose [1] could be implemented. In addition, by extending the loading time for
444 trehalose, the amount of intracellular trehalose increases [56]. However, HepG2 cell spheroids
445 share less total surface area with surrounding media which might reduce the efficacy of given
446 methods.
447
448 Trehalose decreases the phase transition temperature from gel to liquid crystalline of the
449 dry phospholipid membranes [10,12] by replacing the sublimating water molecules [11]
450 according to the water replacement hypothesis. If cells are rehydrated below the phase transition
451 temperature of the phospholipid bilayer, leakage occurs [13]. This might explain the observed
452 leakage in our study with both control cells and cells in native NFC hydrogel. By lowering the
453 transition temperature by inducing higher concentrations of trehalose and rehydrating the HepG2
454 cell spheroids with warm revival solution, the viability of the cells could potentially be increased.
455

456 The rehydration of anhydrobiotic organisms occurs in sections of rapid and a slow
457 imbibition [12]. The results obtained from the rehydration of dry yeast suggest that 20% of water
458 content should be reached inside the cell during prehydration prior to full rehydration [53]. In
459 addition, the optical density of freeze-dried and prehydrated platelets resembled the original
460 optical density [57]. In our study, rapid rehydration of the freeze-dried HepG2 cell spheroids
461 resulted in higher enzymatic activity than when prehydration was implemented. This might be
462 due to collapsing of the freeze-dried cake during the prehydration or the fusion of cell
463 membranes during rehydration. The importance of proper rehydration process has been
464 demonstrated with lactic acid bacteria [16].
465
466 The amount or quality of lyoprotectants in our study was not sufficient in the preservation
467 of actin during freeze-drying. F-actin is present in all human cells and has a significant role in
468 cell signaling, cell attachment, cytokinesis and cell shape. Phalloidin binds specifically to F-actin
469 [58]. Isolated F-actin can be freeze-dried if sucrose and dextran are applied as lyoprotectants [3].
470 In our case, the observed absence of F-actin is in consensus with the observed shrinkage of
471 nuclei in freeze-dried spheroids, as the de-polymerization of F-actin results in shrinkage of nuclei
472 [28]. Moreover, hyperosmotic conditions contribute to the nuclei shrinkage [21,28]. The
473 hyperosmotic conditions can occur briefly during freezing and rehydration. In addition, nuclei
474 size can be affected by hypoxia which causes caspase independent cell death [48]. Hypoxia can
475 occur during freezing and rehydration.
476
477 Surface structures and cell membranes of freeze-dried HepG2 cell spheroids observed with
478 SEM appeared intact and resembled the reference images [36]. It appears that the cell membrane

is intact in the dry state and damaged during the rehydration phase. The freeze-dried HepG2 cell spheroids were integrated as a part of the solid NFC aerogel fiber network. In addition, the observed 3D structure of the freeze-dried HepG2 spheroids appeared intact when NFC was used as a scaffold. The observed hornification in repeated drying cycles is typical to cellulose [20].

Conclusions

Freeze-drying ANFC together with ATE did not change the growth factor release properties of ANFC. The intracellular structures of freeze-dried and rehydrated HepG2 cell spheroids appeared to be partly intact, however the cell membranes were damaged and the cells did not proliferate. The HepG2 cell spheroids showed enzymatic and metabolic activity and the 3D structures of the spheroids were preserved. It appears that the 3D structure of the cell spheroids protects the intracellular structures and functionality of individual cells in the spheroids and not the presence of NFC fibers. The mechanisms of damage were largely recognized which aids in the design of future studies.

Funding sources

This work was supported by the Business Finland and UPM-Kymmene (UPM wound, 3D-NanoMiniT, grant no. 3582/31/2014); Doctoral Programme in Materials Research and Nanosciences; The Osk. Huttunen Foundation; Professor Pool and Academy of Finland (Grant no. 264988, 258114).

The funders had no role in study design, data collection and analysis, decision to publish, or preparation of the manuscript. We have no conflicts of interest to disclose.

Acknowledgements

The authors acknowledge the Drug Discovery and Chemical Biology Network and Institute of Biotechnology for providing access to screening instrumentation, and the Helsinki Electron microscopy unit at the Institute of Biotechnology, University of Helsinki, for the electron microscopy.

References

[1] A. Abazari, L.G. Meimetis, G. Budin, S.S. Bale, R. Weissleder, M. Toner, Engineered Trehalose Permeable to Mammalian Cells, PLoS One 10 (2015) e0130323. doi:10.1371/journal.pone.0130323 [doi].

[2] A. Al-Hussein, H. Gieseler, Investigation of the stabilizing effects of hydroxyethyl cellulose on LDH during freeze drying and freeze thawing cycles, Pharm. Dev. Technol. 20 (2015) 50-59.

[3] S.D. Allison, T.W. Randolph, M.C. Manning, K. Middleton, A. Davis, J.F. Carpenter, Effects of drying methods and additives on structure and function of actin: mechanisms of dehydration-induced damage and its inhibition, Arch. Biochem. Biophys. 358 (1998) 171-181. doi:S0003-9861(98)90832-3 [pii].

[4] M. Antinori, E. Licata, G. Dani, F. Cerusico, C. Versaci, S. Antinori, Cryotop vitrification of human oocytes results in high survival rate and healthy deliveries, Reprod. Biomed. Online 14 (2007) 72-79.

[5] M. Bhattacharya, M.M. Malinen, P. Lauren, Y. Lou, S.W. Kuisma, L. Kanninen, M. Lille, A. Corlu, C. GuGuen-Guillouzo, O. Ikkala, A. Laukkanen, A. Urtti, M. Yliperttula, Nanofibrillar cellulose hydrogel promotes three-dimensional liver cell culture, Journal of controlled release : official journal of the Controlled Release Society 164 (2012) 291-8. doi:10.1016/j.jconrel.2012.06.039.

[6] S. Breslin, L. O'Driscoll, Three-dimensional cell culture: the missing link in drug discovery, Drug Discovery Today 18 (2013) 240-249. doi://doi.org/10.1016/j.drudis.2012.10.003.

[7] P. Carmeliet, Angiogenesis in life, disease and medicine, Nature 438 (2005) 932.

[8] B.M. Cherian, A.L. Leão, S.F. de Souza, S. Thomas, L.A. Pothan, M. Kottaisamy, Isolation of nanocellulose from pineapple leaf fibres by steam explosion, Carbohydr. Polym. 81 (2010) 720-725.

[9] J.H. Crowe, L.M. Crowe, D. Chapman, Preservation of membranes in anhydrobiotic organisms: the role of trehalose, Science 223 (1984) 701-703. doi:223/4637/701 [pii].

[10] J.H. Crowe, J.F. Carpenter, L.M. Crowe, T.J. Anchordoguy, Are freezing and dehydration similar stress vectors? A comparison of modes of interaction of stabilizing solutes with biomolecules, Cryobiology 27 (1990) 219-231. doi://doi.org/10.1016/0011-2240(90)90023-W.

[11] J.H. Crowe, L.M. Crowe, J.F. Carpenter, A.S. Rudolph, C.A. Wistrom, B.J. Spargo, T.J. Anchordoguy, Interactions of sugars with membranes. Biochim. Biophys. Acta 947 (1988) 367-384.

[12] J.H. Crowe, F.A. Hoekstra, L.M. Crowe, Anhydrobiosis, Annu. Rev. Physiol. 54 (1992) 579-599.

[13] J.H. Crowe, F.A. Hoekstra, L.M. Crowe, Membrane phase transitions are responsible for imbibitional damage in dry pollen, Proc. Natl. Acad. Sci. USA 86 (1989) 520-523.

[14] L.M. Crowe, J.H. Crowe, A. Rudolph, C. Womersley, L. Appel, Preservation of freeze-dried liposomes by trehalose, Archives of Biochemistry and Biophysics 242 (1985) 240-247. doi://doi.org/10.1016/0003-9861(85)90498-9.

[15] W.E. Crowe, J. Altamirano, L. Huerto, F.J. Alvarez-Leefmans, Volume changes in single N1E-115 neuroblastoma cells measured with a fluorescent probe, Neuroscience 69 (1995) 283-296. doi:10.1016/0306-4522(95)00219-9.

[16] G.F. De Valdez, G.S. de Giori, de Ruiz Holgado, A Pesce, G. Oliver, Effect of the rehydration medium on the recovery of freeze-dried lactic acid bacteria. Appl. Environ. Microbiol. 50 (1985) 1339-1341.

[17] A. Des Rieux, B. Ucakar, B.P.K. Mupendwa, D. Colau, O. Feron, P. Carmeliet, V. Préat, 3D systems delivering VEGF to promote angiogenesis for tissue engineering, J. Controlled Release 150 (2011) 272-278.

[18] J. Dufresne, T. Hoang, J. Ajambo, A. Florentinus-Mefailoski, P. Bowden, J. Marshall, Freeze-dried plasma proteins are stable at room temperature for at least 1 year, Clinical Proteomics 14 (2017) 35. doi:10.1186/s12014-017-9170-0.

[19] G.M. Fahy, D.R. MacFarlane, C.A. Angell, H.T. Meryman, Vitrification as an approach to cryopreservation, Cryobiology 21 (1984) 407-426.

[20] J. Fernandes Diniz, M. Gil, J. Castro, Hornification—its origin and interpretation in wood pulps, Wood Sci Technol 37 (2004) 489-494. doi:10.1007/s00226-003-0216-2.

[21] J.D. Finan, F. Guilak, The effects of osmotic stress on the structure and function of the cell nucleus, J. Cell. Biochem. 109 (2010) 460-467. doi:10.1002/jcb.22437 [doi].

[22] A. Flood, M. Estrada, D. McAdams, Y. Ji, D. Chen, Development of a Freeze-Dried, Heat-Stable Influenza Subunit Vaccine Formulation, PloS one 11 (2016) e0164692.

[23] X. Fu, L. Fang, H. Li, X. Li, B. Cheng, Z. Sheng, Adipose tissue extract enhances skin wound healing, Wound repair and regeneration 15 (2007) 540-548.

[24] H. He, B. Liu, Z. Hua, C. Li, Z. Wu, Intracellular trehalose improves the survival of human red blood cells by freeze-drying, Front. Energy Power Eng. China 1 (2007) 120-124. doi:10.1007/s11708-007-0014-x.

[25] O. Huttala, M. Palmroth, P. Hemminki, T. Toimela, T. Heinonen, T. Ylikomi, J. Sarkanen, Development of Versatile Human In Vitro Vascularized Adipose Tissue Model with Serum□Free Angiogenesis and Natural Adipogenesis Induction, Basic & clinical pharmacology & toxicology (2018).

[26] A. Jagannath, P.S. Raju, A.S. Bawa, Comparative evaluation of bacterial cellulose (nata) as a cryoprotectant and carrier support during the freeze drying process of probiotic lactic acid bacteria, LWT-Food Science and Technology 43 (2010) 1197-1203.

[27] S.I. Jeon, J.H. Lee, J.D. Andrade, P. De Gennes, Protein—surface interactions in the presence of polyethylene oxide: I. Simplified theory, J. Colloid Interface Sci. 142 (1991) 149-158.

[28] P. Jevtić, L.J. Edens, L.D. Vuković, D.L. Levy, Sizing and shaping the nucleus: mechanisms and significance, Current Opinion in Cell Biology 28 (2014) 16-27. doi://doi.org/10.1016/j.ceb.2014.01.003.

[29] R.A. Jones, A. Smail, M.R. Wilson, Detecting mitochondrial permeability transition by confocal imaging of intact cells pinocytically loaded with calcein, European Journal of Biochemistry 269 (2002) 3990-3997. doi:10.1046/j.1432-1033.2002.03087.x.

592 [30] D. Klemm, F. Kramer, S. Moritz, T. Lindström, M. Ankerfors, D. Gray, A. Dorris,
593 Nanocelluloses: a new family of nature□based materials, Angewandte Chemie International
594 Edition 50 (2011) 5438-5466.

595 [31] R. Koivuniemi, T. Hakkarainen, J. Kiiskinen, M. Kosonen, J. Vuola, J. Valtonen, K.
596 Luukko, H. Kavola, M. Yliperttula, Clinical Study of Nanofibrillar Cellulose Hydrogel Dressing
597 for Skin Graft Donor Site Treatment, Advances in Wound Care (2019).

598 [32] P. Laurén, Y. Lou, M. Raki, A. Urtti, K. Bergström, M. Yliperttula, Technetium-99m-
599 labeled nanofibrillar cellulose hydrogel for in vivo drug release, European Journal of
600 Pharmaceutical Sciences 65 (2014) 79-88.

601 [33] P. Laurén, P. Somersalo, I. Pitkänen, Y. Lou, A. Urtti, J. Partanen, J. Seppälä, M.
602 Madetoja, T. Laaksonen, A. Mäkitie, Nanofibrillar cellulose-alginate hydrogel coated surgical
603 sutures as cell-carrier systems, PLoS One 12 (2017) e0183487.

604 [34] J.F. López, J. Sarkanen, O. Huttala, I.S. Kaartinen, H.O. Kuokkanen, T. Ylikomi,
605 Adipose tissue extract shows potential for wound healing: in vitro proliferation and migration of
606 cell types contributing to wound healing in the presence of adipose tissue preparation and platelet
607 rich plasma, Cytotechnology (2018) 1-12.

608 [35] J. López, O. Huttala, J. Sarkanen, I. Kaartinen, H. Kuokkanen, T. Ylikomi, Cytokine-
609 rich adipose tissue extract production from water-assisted lipoaspirate: methodology for clinical
610 use, BioResearch open access 5 (2016) 269-278.

611 [36] Y. Lou, L. Kanninen, B. Kaehr, J.L. Townson, J. Niklander, R. Harjumäki, C. Jeffrey
612 Brinker, M. Yliperttula, Silica bioreplication preserves three-dimensional spheroid structures of
613 human pluripotent stem cells and HepG2 cells, Scientific reports 5 (2015) 13635.
614 doi:10.1038/srep13635.

615 [37] Y. Lou, A.W. Leung, Next generation organoids for biomedical research and
616 applications, Biotechnol. Adv. (2017).

617 [38] X. Ma, K. Jamil, T.H. MacRae, J.S. Clegg, J.M. Russell, T.S. Villeneuve, M. Euloth,
618 Y. Sun, J.H. Crowe, F. Tablin, A small stress protein acts synergistically with trehalose to confer
619 desiccation tolerance on mammalian cells, Cryobiology 51 (2005) 15-28.

620 [39] M.M. Malinen, L.K. Kanninen, A. Corlu, H.M. Isoniemi, Y. Lou, M.L. Yliperttula,
621 A.O. Urtti, Differentiation of liver progenitor cell line to functional organotypic cultures in 3D
622 nanofibrillar cellulose and hyaluronan-gelatin hydrogels, Biomaterials 35 (2014) 5110-5121.
623 doi:10.1016/j.biomaterials.2014.03.020.

624 [40] D. Natan, A. Nagler, A. Arav, Freeze-Drying of Mononuclear Cells Derived from
625 Umbilical Cord Blood Followed by Colony Formation, PLOS ONE 4 (2009) e5240.

[41] F. Pampaloni, E.G. Reynaud, E.H. Stelzer, The third dimension bridges the gap between cell culture and live tissue, Nature reviews Molecular cell biology 8 (2007) 839.

[42] H. Paukkonen, M. Kunnari, P. Laurén, T. Hakkarainen, V. Auvinen, T. Oksanen, R. Koivuniemi, M. Yliperttula, T. Laaksonen, Nanofibrillar cellulose hydrogels and reconstructed hydrogels as matrices for controlled drug release, International Journal of Pharmaceutics 532 (2017) 269-280. doi://doi.org/10.1016/j.ijpharm.2017.09.002.

[43] S.C. Ramaiahgari, M.W. Den Braver, B. Herpers, V. Terpstra, J.N. Commandeur, B. van de Water, L.S. Price, A 3D in vitro model of differentiated HepG2 cell spheroids with improved liver-like properties for repeated dose high-throughput toxicity studies, Arch. Toxicol. 88 (2014) 1083-1095.

[44] N.C. Rivron, J. Liu, J. Rouwkema, J. de Boer, C. van Blitterswijk, Engineering vascularised tissues in vitro, European cells & materials 15 (2008) 27-40.

[45] T. Saito, S. Kimura, Y. Nishiyama, A. Isogai, Cellulose nanofibers prepared by TEMPO-mediated oxidation of native cellulose, Biomacromolecules 8 (2007) 2485-2491.

[46] T. Saito, Y. Nishiyama, J. Putaux, M. Vignon, A. Isogai, Homogeneous suspensions of individualized microfibrils from TEMPO-catalyzed oxidation of native cellulose, Biomacromolecules 7 (2006) 1687-1691.

[47] J. Sarkanen, V. Kaila, B. Mannerström, S. Räty, H. Kuokkanen, S. Miettinen, T. Ylikomi, Human adipose tissue extract induces angiogenesis and adipogenesis in vitro, Tissue Engineering Part A 18 (2011) 17-25.

[48] K. Shinzawa, Y. Tsujimoto, PL[A.sub.2] activity is required for nuclear shrinkage in caspase-independent cell death, The Journal of Cell Biology 163 (2003) 1219.

[49] Shumin Li, Nilay Chakraborty, Apurva Borcar, Michael A. Menze, Mehmet Toner, Steven C. Hand, Late embryogenesis abundant proteins protect human hepatoma cells during acute desiccation, Proceedings of the National Academy of Sciences of the United States of America 109 (2012) 20859-20864. doi:10.1073/pnas.1214893109.

[50] G.D. Smith, P.C. Serafini, J. Fioravanti, I. Yadid, M. Coslovsky, P. Hassun, J.R. Alegretti, E.L. Motta, Prospective randomized comparison of human oocyte cryopreservation with slow-rate freezing or vitrification, Fertility and Sterility 94 (2010) 2088-2095. doi://doi.org/10.1016/j.fertnstert.2009.12.065.

[51] K. Thompson, P. Dockery, R. Horobin, Predicting and avoiding subcellular compartmentalization artifacts arising from acetoxymethyl ester calcium imaging probes. The case of fluo-3 AM and a general account of the phenomenon including a problem avoidance chart, Biotechnic & Histochemistry 87 (2012) 468-483. doi:10.3109/10520295.2012.703691.

660 [52] J.J. Towey, A.K. Soper, L. Dougan, Molecular Insight Into the Hydrogen Bonding and
661 Micro-Segregation of a Cryoprotectant Molecule, J Phys Chem B 116 (2012) 13898-13904.
662 doi:10.1021/jp3093034.

663 [53] J. Van Steveninck, A.M. Ledeboer, Phase transitions in the yeast cell membrane the
664 influence of temperature on the reconstitution of active dry yeast, Biochimica et Biophysica Acta
665 (BBA) - Biomembranes 352 (1974) 64-70. doi://doi.org/10.1016/0005-2736(74)90179-5.

666 [54] T. Wakayama, R. Yanagimachi, Development of normal mice from oocytes injected
667 with freeze-dried spermatozoa, Nat. Biotechnol. 16 (1998) 639.

668 [55] W. Wang, Lyophilization and development of solid protein pharmaceuticals,
669 International Journal of Pharmaceutics 203 (2000) 1-60. doi:10.1016/S0378-5173(00)00423-3.

670 [56] J. Wikström, M. Elomaa, L. Nevala, J. Räikkönen, P. Heljo, A. Urtti, M. Yliperttula,
671 Viability of freeze dried microencapsulated human retinal pigment epithelial cells, European
672 journal of pharmaceutical sciences : official journal of the European Federation for
673 Pharmaceutical Sciences 47 (2012) 520-526. doi:10.1016/j.ejps.2012.06.014.

674 [57] W.F. Wolkers, N.J. Walker, F. Tablin, J.H. Crowe, Human Platelets Loaded with
675 Trehalose Survive Freeze-Drying, Cryobiology 42 (2001) 79-87. doi:10.1006/cryo.2001.2306.

676 [58] E. Wulf, A. Deboben, F.A. Bautz, H. Faulstich, T. Wieland, Fluorescent phallotoxin, a
677 tool for the visualization of cellular actin, Proc. Natl. Acad. Sci. U. S. A. 76 (1979) 4498-4502.

678 [59] M. Zhang, H. Oldenhof, H. Sieme, W.F. Wolkers, Freezing-induced uptake of
679 trehalose into mammalian cells facilitates cryopreservation, Biochimica et Biophysica Acta
680 (BBA) - Biomembranes 1858 (2016) 1400-1409. doi://doi.org/10.1016/j.bbamem.2016.03.020.

681 [60] M. Zhang, H. Oldenhof, B. Sydykov, J. Bigalk, H. Sieme, W.F. Wolkers, Freeze-
682 drying of mammalian cells using trehalose: preservation of DNA integrity, Scientific reports 7
683 (2017) 6198.

684

Fig 1. Preparation and the setup of the release studies. (A) Two 10 ml syringes were connected with an autoclaved rubber hose to mix and homogenize the ATE, the ANFC hydrogel and the lyoprotectants. (B) New syringes were cut open and filled with 1 ml of the mixture of the ANFC hydrogel (3% (m/v) and the ATE and 500 µl of DPBS was carefully added on top as a separate layer. (C) The cut syringes were sealed with aluminum foil and kept at 37 °C on a moving plate shaker for 6 and 24 hours.

Fig 2. Release profiles of growth factors and formed solid end product cakes. (A) The release profiles of IL-6 and VEGF-A from the mixtures of ATE, ANFC hydrogel and lyoprotectants before and after freeze-drying (FD) and rehydration. The error bars represent the range of measured values (n=6). (B) Freeze-dried ATE and mixtures of ATE, ANFC aerogel and lyoprotectants (LP).

Fig 3. The viability of HepG2 cell spheroids after 24 hours of trehalose loading. Viability was determined by Calcein AM (green) and PI (red) staining. Used trehalose concentrations: (A) 0 mM, (B) 50 mM, (C) 100 mM, (D) 200 mM and (E) 500 mM. (F) Viability of the HepG2 cell spheroids decreased as the concentration of trehalose was increased. Origin set to 100 mM. Image of 1000 mM not shown.

Fig 4. HepG2 cell spheroids freeze-dried in 0.4% native NFC hydrogel with different concentrations of trehalose. Cell membrane integrity determined by Calcein AM (green) and PI (red) staining. (A) no trehalose, (B) 50 mM trehalose and (C) 300 mM trehalose. The spheroids freeze-dried after the incubation in 300 mM trehalose media showed higher intensity of green fluorescence.

Fig 5. Comparison of stained permeabilized control cells and freeze-dried HepG2 cell spheroids. HepG2 cell spheroids were stained with Calcein AM (green) and PI (red). Freeze-dried, rehydrated and stained spheroids, (A) at 40 °C and (B) at 4°C, (C) control cells

permeabilized with Triton X-100 before staining and (D) control cells stained and simultaneously permeabilized with Triton X-100. Freeze-dried spheroids stained with calcein AM had similar granular bright spots and lower overall intensity as the control cells which were permeabilized with Triton X-100.

Fig 6. Metabolic activity and morphology of HepG2 cell spheroids. (A) Metabolic activity of the HepG2 cell spheroids during the 14-days experiment period. Fluorescence values are normalized to the fluorescence of the control cells at day 1. The cell spheroids were freeze-dried on day 4 (marked with a dashed line). Error bars: 95% CI, n=8. (B) A control HepG2 cell spheroid stained with phalloidin Alexa 488 and Hoechst 33342. (C) A freeze-dried and rehydrated HepG2 cell spheroid stained with phalloidin Alexa 488 and Hoechst 33342.

Fig 7. SEM images of freeze-dried HepG2 cell spheroids in native NFC aerogel without fixing nor coating. (A) A HepG2 cell spheroid integrated in native NFC aerogel. (B) A zoomed image of the same spheroid. (C) A single HepG2 cell showing surface structures. (D) Freeze-dried and rehydrated native NFC hydrogel after refreeze-drying demonstrating the lack of detectable cells.

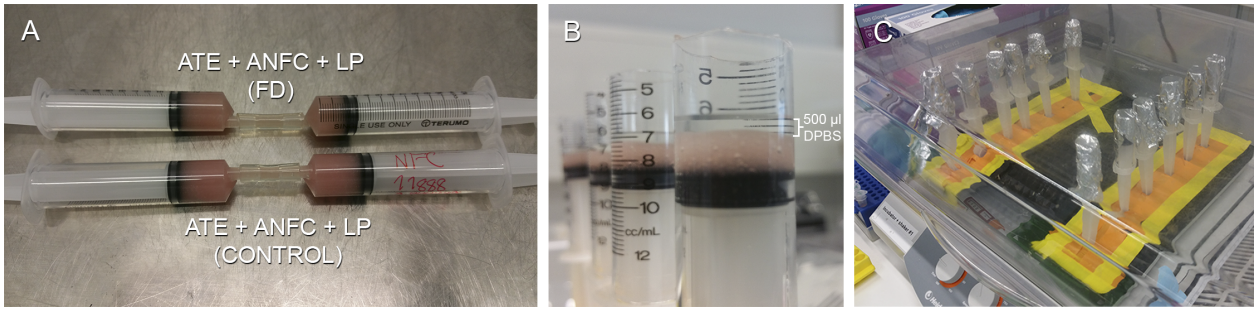

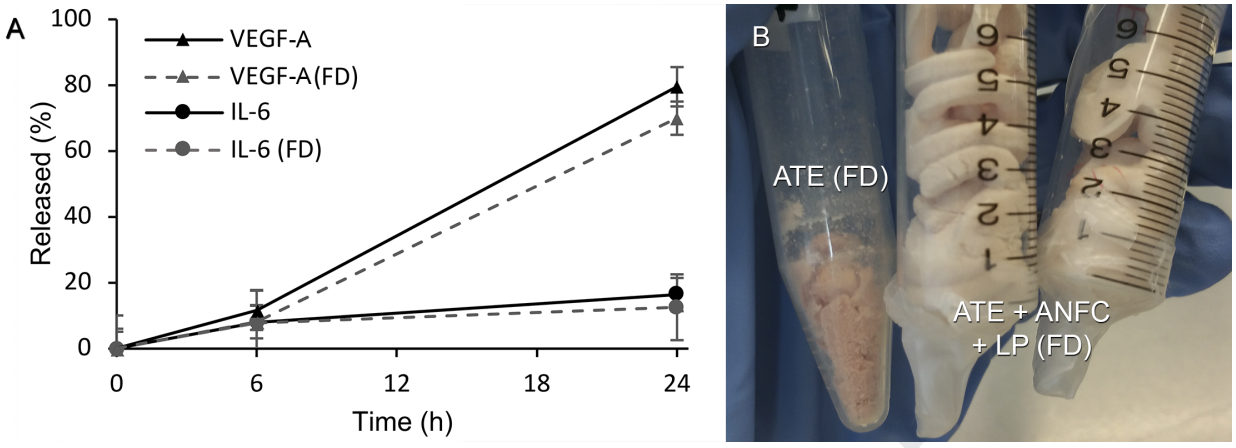

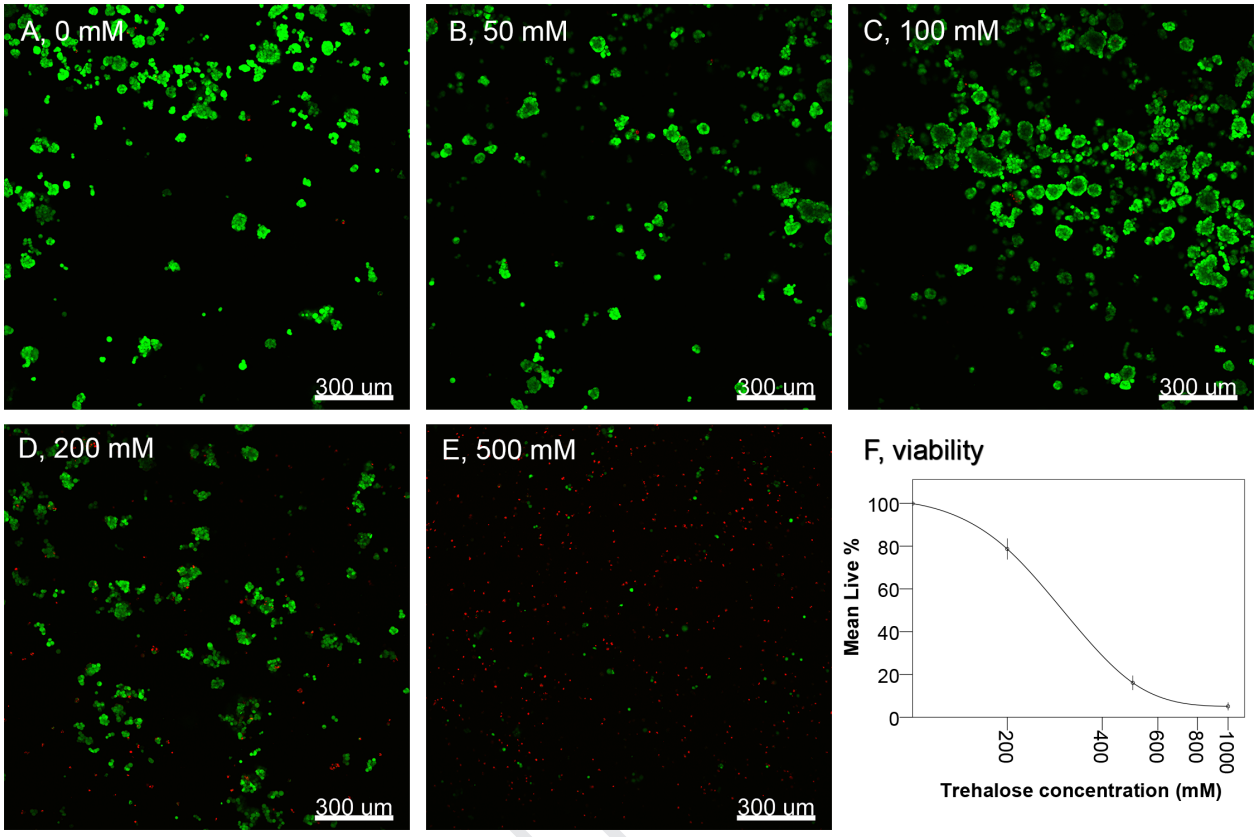

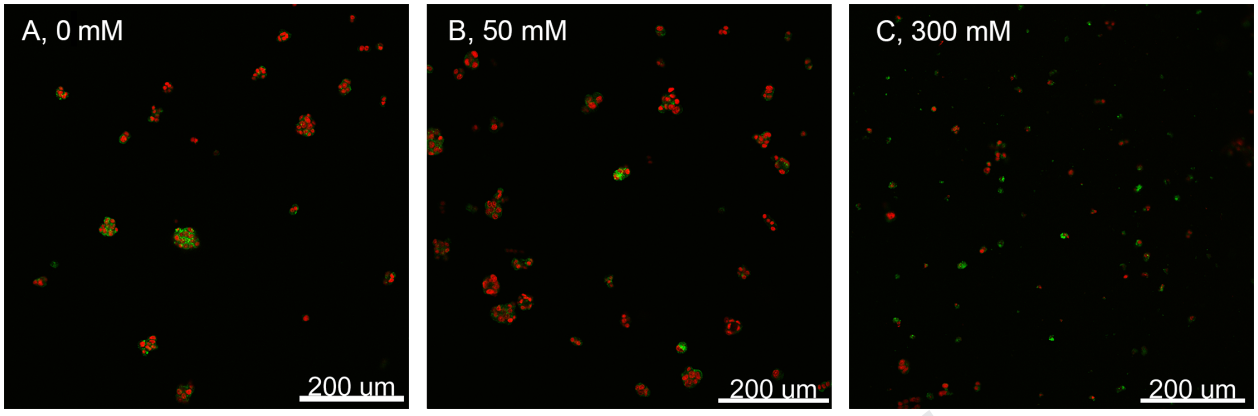

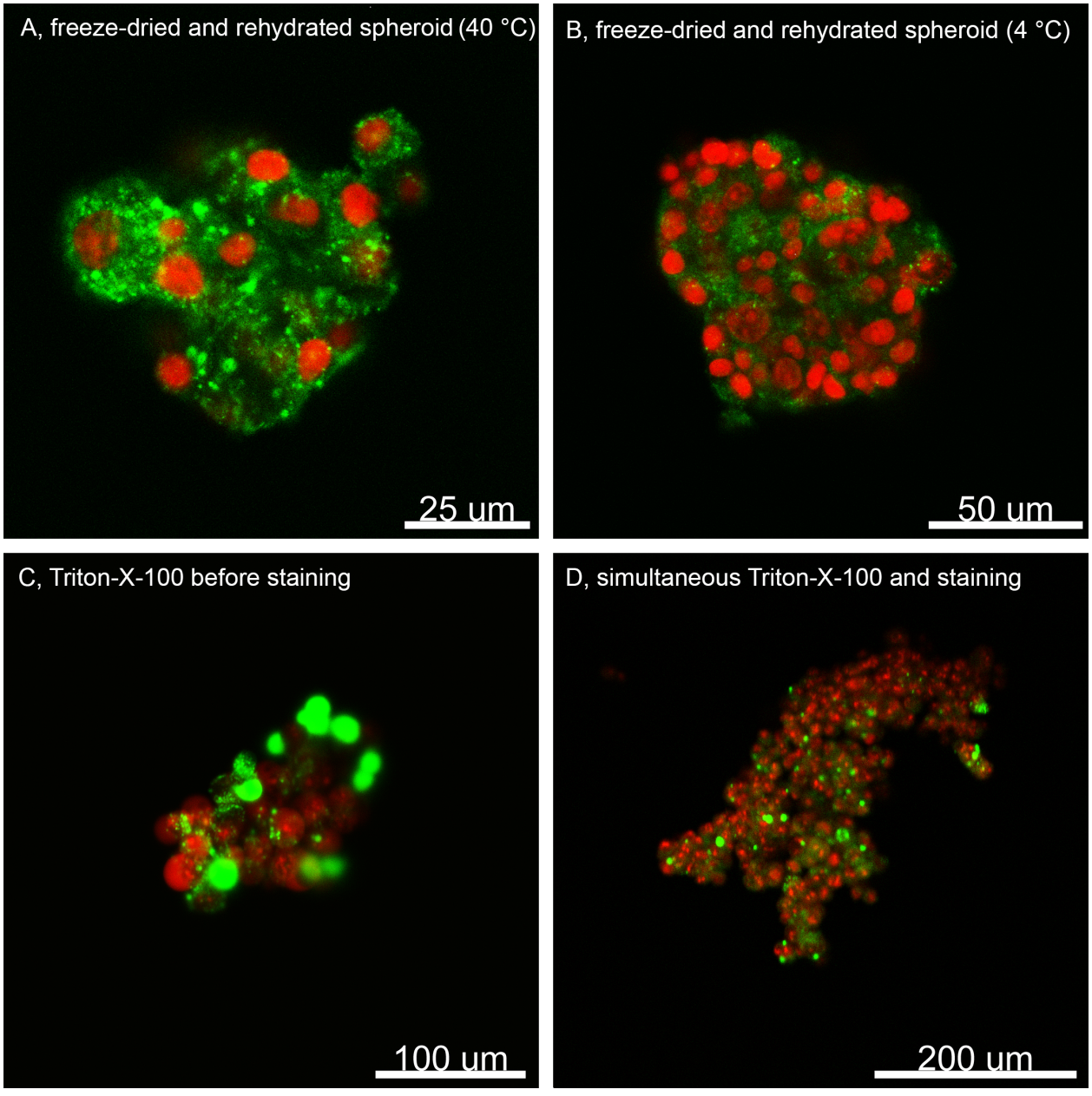
A, freeze-dried and rehydrated spheroid (40 °C)
25 um
B, freeze-dried and rehydrated spheroid (4 °C)
50 um
C, Triton-X-100 before staining
100 um
D, simultaneous Triton-X-100 and staining
200 um

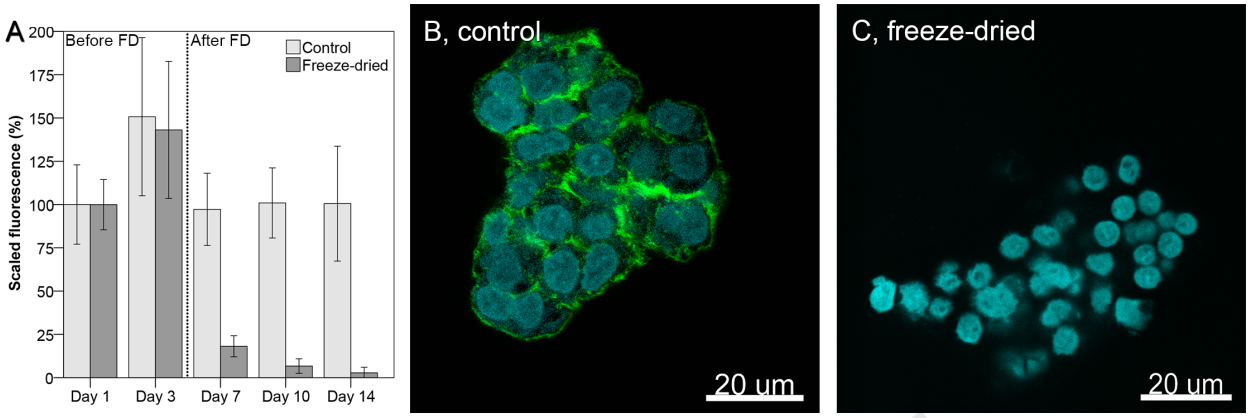

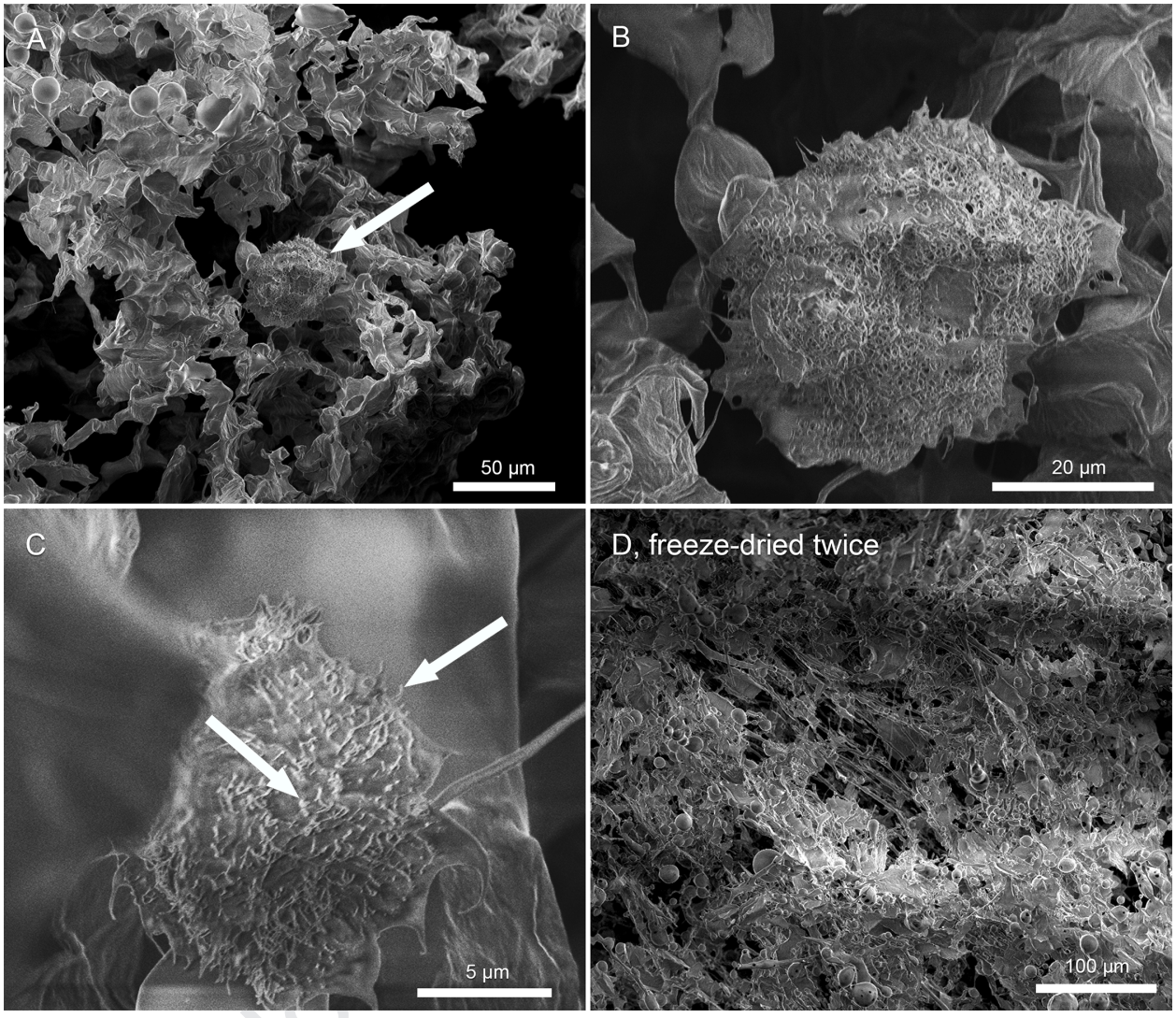
A
50 µm
B
20 µm
C
5 µm
D, freeze-dried twice
100 µm